NEURAL REGENERATION RESEARCH
October 2015, Volume 10, Issue 10
www.nrronline.org

RESEARCH ARTICLE

Neuroprotective effects of electroacupuncture on early- and late-stage spinal cord injury

Min-fei Wu[1], Shu-quan Zhang[2], Jia-bei Liu[3], Ye Li[3], Qing-san Zhu[3], Rui Gu[3, *]

1 Department of Orthopedics, Bethune Second Hospital of Jilin University, Changchun, Jilin Province, China
2 Department of Orthopedics, Tianjin Nankai Hospital, Tianjin, China
3 Department of Orthopedics, China-Japan Union Hospital, Jilin University, Changchun, Jilin Province, China

***Correspondence to:**
Rui Gu, M.D., fandiliucl@126.com.

orcid:
0000-0003-4406-1553 (Rui Gu)

doi: *10.4103/1673-5374.167762*
http://www.nrronline.org/

Accepted: *2015-08-21*

Abstract

Previous studies have shown that the neurite growth inhibitor Nogo-A can cause secondary neural damage by activating RhoA. In the present study, we hypothesized that electroacupuncture promotes neurological functional recovery after spinal cord injury by inhibiting RhoA expression. We established a rat model of acute spinal cord injury using a modification of Allen's method. The rats were given electroacupuncture treatment at *Dazhui* (Du14), *Mingmen* (Du4), *Sanyinjiao* (SP6), *Huantiao* (GB30), *Zusanli* (ST36) and *Kunlun* (BL60) acupoints with a sparse-dense wave at a frequency of 4 Hz for 30 minutes, once a day, for a total of 7 days. Seven days after injury, the Basso, Beattie and Bresnahan (BBB) locomotor scale and inclined plane test scores were significantly increased, the number of apoptotic cells in the spinal cord tissue was significantly reduced, and RhoA and Nogo-A mRNA and protein expression levels were decreased in rats given electroacupuncture compared with rats not given electroacupuncture. Four weeks after injury, pathological tissue damage in the spinal cord at the site of injury was alleviated, the numbers of glial fibrillary acidic protein- and neurofilament 200-positive fibers were increased, the latencies of somatosensory-evoked and motor-evoked potentials were shortened, and their amplitudes were increased in rats given electroacupuncture. These findings suggest that electroacupuncture treatment reduces neuronal apoptosis and decreases RhoA and Nogo-A mRNA and protein expression at the site of spinal cord injury, thereby promoting tissue repair and neurological functional recovery.

Key Words: *nerve regeneration; spinal cord injury; electroacupuncture; locomotion; RhoA; Nogo-A; glial fibrillary acidic protein; neurofilament 200; neural regeneration*

Funding: *This study was supported by a grant from the Science and Technology Development Program of Jilin Province of China, No. 2011084.*

Wu MF, Zhang SQ, Liu JB, Li Y, Zhu QS, Gu R (2015) Neuroprotective effects of electroacupuncture on early- and late-stage spinal cord injury. Neural Regen Res 10(10):1628-1634.

Introduction

Recovery of motor function after spinal cord injury (SCI) is currently the most important step in clinical rehabilitative treatment (Parikh et al., 2011). Spinal cord neurons are non-renewable, and while slow recovery of injured spinal cord neurons and neurite outgrowth can be achieved, regeneration and functional recovery are limited because of irreversible pathophysiological processes after SCI (Ding et al., 2011). There is strong evidence that electroacupuncture greatly promotes the recovery of locomotor function after SCI (Davies et al., 2011; Huang et al., 2011; Li et al., 2011; Oyinbo, 2011). Electroacupuncture treatment substantially decreases aquaporin-4 and monocyte chemoattractant protein 1 (MCP-1) expression, alleviates spinal cord inflammation and edema, and protects against secondary injury (Xie et al., 2013). Li et al. (2015) performed electroacupuncture at *Dazhui* (DU14), *Mingmen* (DU4), *Sanyinjiao* (SP6), *Huantiao* (GB30), *Zusanli* (ST36) and *Kunlun* (BL60) acupoints after SCI, and achieved striking recovery of motor and sensory function.

Electroacupuncture treatment can reduce pain after SCI, and its combined application with medication and physical therapy can promote the recovery of motor, sensory and electrophysiological function (Xie et al., 2013). Nogo-A is a neurite growth inhibitor found in myelin in the central nervous system that has been found to cause secondary brain damage by activating RhoA (Jiang et al., 2009). In this study, we investigated whether electroacupuncture treatment affects RhoA and Nogo-A expression in a rat model of SCI.

Materials and Methods

Ethics statement

All experimental protocols were approved by the Animal Ethics Committee, Bethune Second Hospital of Jilin University, China. The animal studies were performed in accordance with the National Institutes of Health Guide for the Care and Use of Laboratory Animals. Precautions were taken to minimize suffering and the number of animals used in each experiment.

SCI model establishment

Sixty-eight clean female Sprague-Dawley rats, 7 weeks of age, weighing 250–290 g, were purchased from the Laboratory Animal Center, Tianjin Medical University, China (license No. SCXK (Jin) 20090001). All rats were intraperitoneally anesthetized with 10% chloral hydrate (350 mg/kg). A median incision was made on the back to fully expose the $T_{8–11}$ spinous processes and the vertebral plate. After removal of the $T_{9–10}$ spinous processes and a part of the vertebral plate, the dura mater was exposed, but left intact. According to a modification of Allen's method (Allen, 1911), a 10-g object was dropped from a vertical height of 2.5 cm, directly impacting the dura mater and spinal cord. Paralysis of the hindlimbs was observed after impact as the swinging and spasmodic contraction of the tail, suggesting successful establishment of the SCI model. Wounds were washed with penicillin/saline, and the tissue was sutured closed layer by layer. After injury, lower abdominal massage was performed twice or three times to assist urination. Rats (n = 20) in the sham-operated group were only subjected to exposure of the spinal cord. Five rats were rejected for lack of successful SCI, and three rats died after SCI. The remaining 40 rats were randomly and evenly divided into a SCI group and an electroacupuncture group.

Electroacupuncture treatment

Six hours after SCI, rats underwent electroacupuncture treatment. Stainless steel needles (1 cun, diameter 0.5 mm; Beijing Sishengda Medical Equipment Center, China) were inserted at *Dazhui* (DU14; located below the spinous process of C_7; downward oblique needling) and *Mingmen* (DU4; located below the spinous process of L_2; upward oblique needling) to a depth of 0.5–0.6 cm. *Sanyinjiao* (SP6; located in the inner side of the hindlimbs and 10 mm above the ankle; vertical needling to a depth of 4–5 mm), *Huantiao* (GB30; located at the posterior upper border of the hip joint of the hindlimbs; vertical needling to a depth of 6 mm), *Zusanli* (ST36; 5 mm below the head of the fibula under the knee joint, and 2 mm lateral to the knee joint; vertical needling to a depth of 6 mm) and *Kunlun* (BL60; located at the ankle joint level between the external malleolus and the tendo calcaneus in the hindlimb; vertical needling to a depth of 3 mm) were also simultaneously punctured. An electroacupuncture apparatus (Model G-6805-1, Qingdao Xinsheng Industrial Co., Ltd., Qingdao, Shandong Province, China) was used, with a sparse-dense wave at a frequency of 4 Hz, for 30 minutes once a day, for a total of 7 days. Stimulation intensity was regulated within a range of 0.3–0.6 mA, taking a slight vibration of the hindlimb as an indicator.

Locomotor function evaluation

Before, 1 and 3 days, and 1, 2, 3 and 4 weeks after injury, locomotor function of the hindlimbs was scored using a modified Basso, Beattie and Bresnahan (BBB) locomotor scale (Wang et al., 2013) and the inclined plane test (Wang and Zhang, 2015). The range of BBB scores was between 0 (complete paralysis) and 21 (normal). The extent and range of motion, weight loading, coordination of the forelimb and hindlimb, and motion of the forepaw, hindpaw and tail were evaluated. For the inclined plane test, the rats were placed horizontally on a smooth tilted board. From the horizontal position (0°), the angle of the board was increased in 5° increments. The maximum angle at which the rat remained on the board for a minimum of 5 minutes was recorded.

Detection of cellular apoptosis by TUNEL

Seven days after SCI, five rats were selected from each group. After anesthesia with chloral hydrate, aortic cannulation through the apex of the left ventricle was performed *via* thoracotomy, and the heart was fixed with 4% paraformaldehyde. A 2.0-cm length of spinal cord tissue centered at the site of SCI (T_{10}) was harvested, fixed with paraformaldehyde, paraffin embedded, sliced into 5-μm-thick sections, dewaxed, dehydrated through a graded ethanol series, treated with proteinase K solution for 10 minutes at room temperature, and washed three times with PBS. Sections were then incubated with TUNEL reagent (Roche, Basel, Switzerland) at 37°C for 1 hour, treated with 3% H_2O_2/methanol for 10 minutes at room temperature, washed three times with PBS, incubated with peroxidase at 37°C for 30 minutes, washed three times with PBS, and developed with diaminobenzidine. Thereafter, the sections were washed three times with PBS, counterstained with hematoxylin-eosin, dehydrated through a graded ethanol series, cleared with xylene, mounted with neutral gum, and observed under an optical microscope (Shenzhen Mashide Instrument Co., Ltd., China). Ten fields at 200× magnification were selected from each rat, and the mean value across the 10 fields was calculated.

Reverse transcription PCR

Seven days after SCI, five rats were selected from each group and 50 g of spinal cord tissue was harvested from the injured region. According to the manufacturer's instructions, Trizol reagent (Invitrogen Life Technologies, Carlsbad, CA, USA) was used to extract total RNA from spinal cord tissue, and total RNA content was measured using an ultraviolet spectrophotometer (Shanghai Puyuan Instrument Co., Ltd., China). mRNA was reverse transcribed into cDNA using RT-PCR (Takara Biotechnology (Dalian) Co., Ltd., China). RhoA, Nogo-A and β-actin cDNAs were amplified using the following primers:

Gene	Primer sequence (5′–3′)	Product size (bp)	Temperature (°C)
β-Actin	Upstream: CCA TCA TGA AGT GTG ACG TTG Downstream: ACA GAG TAC TTG CGC TCA GGA	175	55
RhoA	Upstream: AAT GTG CCC ATC ATC CTA GTT Downstream: TGT TTG CCA TAT CTC TGC CTT	128	55
Nogo-A	Upstream: GCC TAT TCC TGC TGC TTT CAT T Downstream: TGC CTG ATG CCG TTC ATA AAT A	410	55

Table 1 Effects of electroacupuncture on locomotor function in rats with spinal cord injury (SCI)

Group	Before injury	After injury					
		1 day	3 days	1 week	2 weeks	3 weeks	4 weeks
BBB score							
SCI	21.00±0.00	0.00±0.00	1.32±0.11	2.53±0.72	7.52±1.28$^{\#}$	11.12±1.21$^{\#}$	13.76±0.64$^{\#}$
Electroacupuncture	21.00±0.00	0.00±0.00	2.45±0.12	3.94±1.32*	10.23±2.32$^{*\#}$	12.62±1.74$^{*\#}$	15.22±0.10$^{*\#}$
Sham-operated	21.00±0.00	19.23±0.14	20.14±0.16	20.32±0.45*	20.45±0.43*	20.53±0.21*	21.00±0.00*
Inclined plane test (°)							
SCI	42.50±2.44	15.98±1.74	16.64±1.48	21.54±2.63	22.89±1.45$^{\#}$	25.87±2.45$^{\#}$	28.21±1.43$^{\#}$
Electroacupuncture	42.50±2.56	16.34±2.83	18.92±1.45	24.39±2.18*	29.32±2.45$^{*\#}$	34.67±2.21$^{*\#}$	38.62±2.23$^{*\#}$
Sham-operated	42.50±2.34	40.82±3.12	41.43±2.32	42.32±2.54*	42.42±2.14*	42.35±1.63*	42.48±2.32*

Lower BBB and inclined plane test scores indicate poorer locomotor function. Data are expressed as the mean ± SD of five rats per group per time point. One-way analysis of variance was used for mean comparisons among groups, and two-sample *t*-test for mean comparisons between two groups. *$P < 0.05$, *vs.* SCI group; #$P < 0.05$, *vs.* sham-operated group. BBB: Basso, Beattie and Bresnahan locomotor scale.

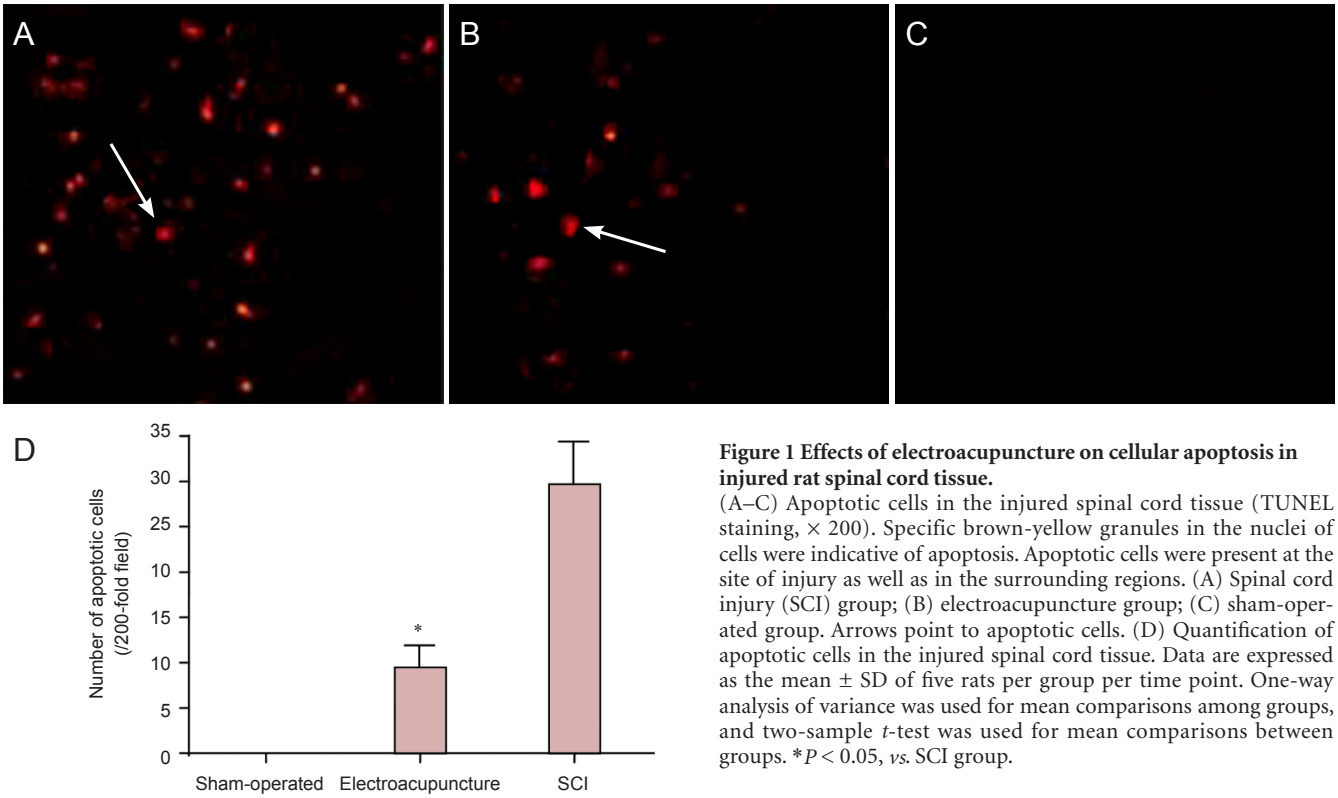

Figure 1 Effects of electroacupuncture on cellular apoptosis in injured rat spinal cord tissue.
(A–C) Apoptotic cells in the injured spinal cord tissue (TUNEL staining, × 200). Specific brown-yellow granules in the nuclei of cells were indicative of apoptosis. Apoptotic cells were present at the site of injury as well as in the surrounding regions. (A) Spinal cord injury (SCI) group; (B) electroacupuncture group; (C) sham-operated group. Arrows point to apoptotic cells. (D) Quantification of apoptotic cells in the injured spinal cord tissue. Data are expressed as the mean ± SD of five rats per group per time point. One-way analysis of variance was used for mean comparisons among groups, and two-sample *t*-test was used for mean comparisons between groups. *$P < 0.05$, *vs.* SCI group.

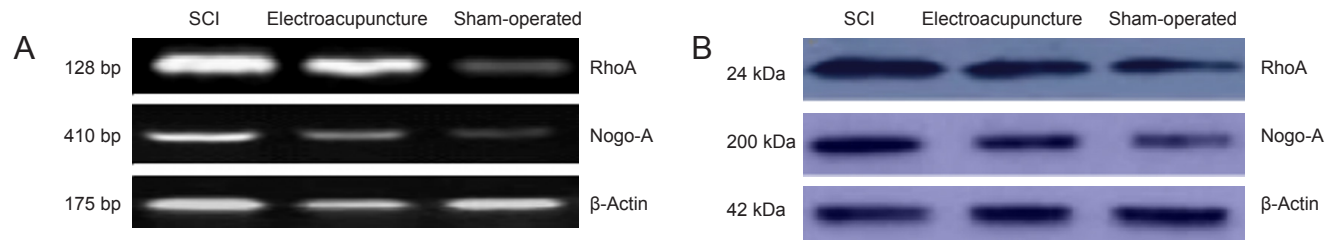

Figure 2 Effects of electroacupuncture on RhoA and Nogo-A mRNA and protein expression levels in injured rat spinal cord tissue.
(A) RhoA and Nogo-A mRNA. (B) RhoA and Nogo-A protein. SCI: Spinal cord injury.

Table 2 Effects of electroacupuncture on RhoA and Nogo-A mRNA and protein expression in injured rat spinal cord tissue

	RhoA		Nogo-A	
Group	mRNA	Protein	mRNA	Protein
SCI	1.75±0.23	1.86±0.22	0.84±0.05	1.27±0.17
Electroacupuncture	1.22±0.16*#	1.21±0.14*#	0.42±0.04*#	0.96±0.12*#
Sham-operated	0.51±0.05	0.83±0.07	0.21±0.02	0.51±0.08

mRNA and protein expression are expressed as the integrated optical density of the target gene mRNA or protein to β-actin mRNA or protein. Data are expressed as the mean ± SD of five rats per group per time point. One-way analysis of variance was used for mean comparisons among groups and two-sample *t*-test for mean comparisons between groups. *$P < 0.05$, *vs.* SCI group, #$P < 0.05$, *vs.* sham-operated group. SCI: spinal cord injury.

Table 3 Effects of electroacupuncture on NF-200 and GFAP-positive cell numbers (/200-fold field) in the injured rat spinal cord

Group	NF-200	GFAP
Sham-operated	12.24±2.82	7.54±3.72
Electroacupuncture	34.54±3.74*	25.84±3.63*
SCI	20.64±3.24	14.42±2.27

Data are expressed as the mean ± SD of five rats per group per time point. One-way analysis of variance was used for mean comparisons among groups, and two-sample *t*-test was used for mean comparisons between two groups.*$P < 0.05$, *vs.* SCI group. NF-200: Neurofilament-200; GFAP: glial fibrillary acidic protein; SCI: spinal cord injury.

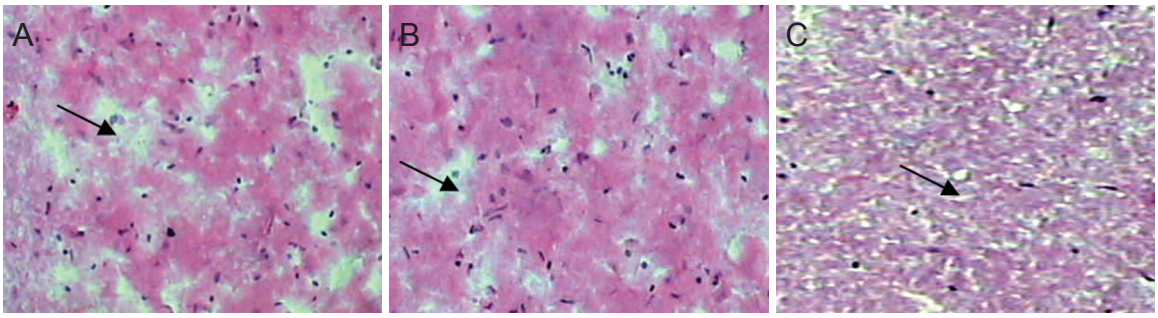

Figure 3 Effects of electroacupuncture on the histopathology of the spinal cord 4 weeks after injury (hematoxylin-eosin staining, × 40).
(A) In the sham-operated group, no spinal cord cavities or apoptotic cells were observed in the spinal cord. (B) In the electroacupuncture group, cavities were small, and only a few apoptotic cells were present. (C) In the spinal cord injury group, substantial spinal cord cavities were observed. Arrows indicate cavities in the spinal cord.

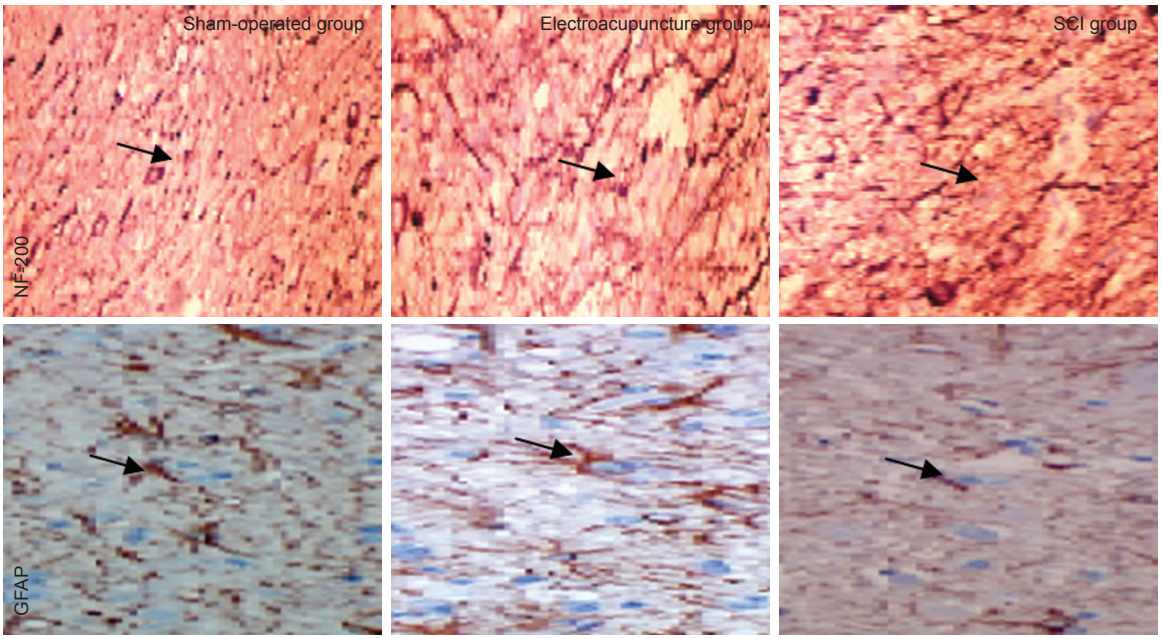

Figure 4 Effects of electroacupuncture on NF-200 and GFAP-positive cells in the injured rat spinal cord (immunofluorescence staining, × 200).
In the sham-operated group, neural fibers in the spinal cord tissue were densely arranged, while in the SCI group, the fibers were sparsely arranged. In the electroacupuncture group, fiber arrangement was substantially improved compared with the SCI group. Yellow arrows point to NF-200 or GFAP-positive fibers. NF-200: Neurofilament-200; GFAP: glial fibrillary acidic protein; SCI: spinal cord injury.

Table 4 Effects of electroacupuncture on nerve conduction in the injured rat spinal cord

	Somatosensory evoked potential		Motor-evoked potential	
Group	Latency (ms)	Amplitude (μV)	Latency (ms)	Amplitude (μV)
SCI	35.143±1.276	1.323±0.143	15.734±0.345	1.643±0.112
Electroacupuncture	26.232±0.865*#	1.743±0.143*#	12.927±0.343*#	2.462±0.263*#
Sham-operated	18.232±0.634	2.108±0.123	8.546±0.123	3.653±0.276

Data are expressed as the mean ± SD of five rats per group per time point. One-way analysis of variance was used for mean comparisons among groups, and two-sample *t*-test for mean comparisons between two groups. *$P < 0.05$, *vs.* SCI group; #$P < 0.05$, *vs.* sham-operated group. SCI: Spinal cord injury.

Amplified products were subjected to electrophoresis, and optical density was analyzed using an image analysis system (Beijing Wuyejia Science and Technology Co., Ltd., China). The integrated optical density ratios of RhoA and Nogo-A to β-actin were calculated and used to determine the respective mRNA expression levels.

Western blot analysis

After Trizol extraction, the remaining fraction was centrifuged at 1,500 r/min for 30 minutes. The supernatant was used for total protein concentration determination using the Bradford method (Yang et al., 2010). The protein samples were electrophoresed on a 10% SDS-PAGE resolving gel and transferred onto a polyvinylidene difluoride membrane at 14 V for 14 hours. Then, the membrane was blocked for 2 hours at 37°C, washed in TBS three times for 10 minutes each, and treated with rabbit anti-rat RhoA monoclonal antibody (1:800; Santa Cruz Biotechnology, Santa Cruz, CA, USA) or rabbit anti-rat β-actin monoclonal antibody (1: 500; Santa Cruz Biotechnology) at 4°C overnight. Thereafter, the membrane was washed in TBST four times for 5 minutes each and incubated with goat anti-rabbit IgG (1:700; Santa Cruz Biotechnology) at 37°C for 1.5 hours, washed in TBST four times for 5 minutes each, in TBS for 10 minutes, and developed with 3,3′-diaminobenzidine (DAB). Optical density ratios of RhoA and Nogo-A to β-actin were determined using Quantify One software (Bio-Rad, Hercules, CA, USA) to calculate the respective protein expression levels.

Immunohistochemical and hematoxylin-eosin staining

Four weeks after SCI, five rats per group were selected. Following anesthesia with 10% chloral hydrate (350 mg/kg), thoracotomy was performed, and the heart was perfused with physiological saline and paraformaldehyde. An approximately 1-cm-long segment of spinal cord tissue encompassing the site of injury (T_{10}) was harvested and dehydrated through a graded ethanol series, and longitudinally sliced into 20-μm-thick sections. Sections were left at room temperature for 30 minutes, blocked with fetal bovine serum for 1 hour, washed three times with PBS for 5 minutes each, and treated with mouse anti-rat monoclonal GFAP antibody (1:100; Sigma-Aldrich, St. Louis, MO, USA) or mouse anti-rat neurofilament (NF)-200 monoclonal antibody (1:100; Sigma) at 4°C overnight. Sections were then washed three times with PBS for 5 minutes each, treated with goat anti-mouse monoclonal secondary antibody (1:500; Amresco Inc., Solon, OH, USA) at 37°C for 2 hours, washed three times with PBS for 5 minutes each, and developed with DAB for 5–10 minutes. Thereafter, the sections were dehydrated through a graded ethanol series, cleared with xylene, and mounted with neutral gum. Image analysis was performed using Image-Pro Plus 6.0 software (Media Cybernetics, Silver Spring, MD, USA). Ten fields, at 200× magnification, were selected from each rat for counting NF-200 and GFAP-positive fibers, and their mean values across 10 fields were calculated. Sections were then stained with hematoxylin-eosin for 5 minutes, washed with running water, treated with HCl/ethanol for 10 seconds, washed with running water for 10 minutes, stained with eosin for 7 minutes, washed with running water, dehydrated through a graded ethanol series, cleared with xylene and mounted with neutral gum. Tissue repair was observed under an optical microscope (Olympus IX71, Olympus Optical Co., Ltd., Tokyo, Japan).

Detection of somatosensory-evoked potentials (SEPs) and motor-evoked potentials (MEPs)

Four weeks after injury, five rats per group were selected. Rat SEP and MEP latencies and amplitudes were detected using a KEYPOINT 4 evoked potential instrument (Natus, San Carlos, CA, USA) according to a previously described method (Wang and Zhang, 2012).

SEP detection: Following anesthesia by intraperitoneal injection of 10% chloral hydrate (350 mg/kg), rats were placed on a horizontal wood plate and a stimulating electrode was fixed onto the hindlimb. The recording electrode was positioned in the corresponding cortical sensory region (beneath the scalp near the intersection of the coronal and sagittal sutures). The reference electrode was placed 0.5 cm posterior to the recording electrode.

Direct-current square wave electrical pulse stimulation was given until the hindlimb exhibited a slight twitch at a current intensity of 5–15 mA, wave width of 0.2 ms, and frequency of 3 Hz, which was repeated 50–60 times. SEP latencies and amplitudes were recorded.

MEP detection: Following anesthesia by intraperitoneal injection of 10% chloral hydrate (350 mg/kg), rats were placed on a horizontal wooden plate. The stimulating electrode was fixed in the cortical motor area (beneath the scalp, 2 mm anterior to the coronal suture and 2 mm lateral to the sagittal suture). The recording electrode was positioned on the sciatic nerve of the hindlimb. Direct-current square wave electrical pulse stimulation was given at a current intensi-

ty of 40 mA, wave width of 0.1 ms, and frequency of 1 Hz, which was repeated 300–500 times. Scanning sensitivity was 5 μV and scanning speed was 5 ms. MEP latencies and amplitudes were recorded.

Statistical analysis

All data are expressed as the mean ± SD and were statistically analyzed using SPSS 17.0 software (SPSS, Chicago, IL, USA). One-way analysis of variance was used for comparison among groups, and two-sample *t*-test for comparison between groups. $P < 0.05$ was considered statistically significant.

Results

Electroacupuncture improves locomotor function in rats with SCI

Prior to SCI, the BBB scores and inclined plane test results were similar among all groups ($P > 0.05$). Two to four weeks after injury, the BBB and inclined plane rest scores in the SCI and electroacupuncture groups were significantly lower than in the sham-operated group ($P < 0.05$). Compared with the SCI group, the BBB and inclined plane rest scores were significantly increased in the electroacupuncture group ($P < 0.05$; **Table 1**).

Electroacupuncture inhibits apoptosis in the injured spinal cord

TUNEL results revealed the absence of apoptotic cells in the spinal cord tissue in rats in the sham-operated group. The number of apoptotic cells in spinal cord tissue was significantly lower in the electroacupuncture group compared with the SCI group ($P < 0.05$; **Figure 1**).

Electroacupuncture inhibits RhoA and Nogo-A mRNA and protein expression in injured spinal cord

RT-PCR and western blot analysis showed that RhoA and Nogo-A mRNA and protein expression levels in the injured spinal cord tissue were significantly lower in the electroacupuncture group than in the SCI group, but significantly greater than in the sham-operated group ($P < 0.05$; **Figure 2**, **Table 2**).

Electroacupuncture alleviates tissue damage in the injured spinal cord

Four weeks after SCI, hematoxylin-eosin staining showed that in the sham-operated group, spinal cord tissue had a complete and clear structure, with no cavities or apoptotic neurons. In the SCI group, spinal cord tissue appeared sparse, with cavities and a large number of necrotic cells. In the electroacupuncture group, cavities were small, and necrotic cells were few (**Figure 3**).

Electroacupuncture promotes regeneration of fibers in the injured spinal cord

In the spinal cord, NF-200 is mainly expressed in neurons (cell membrane and cytoplasm), while GFAP is mainly expressed in astrocytes (cell membrane and cytoplasm) (Qiao et al., 2008). Immunohistochemical staining showed that in the sham-operated group, fibers in the spinal cord were densely arranged, while in the SCI group, they were less compact, and only a few short fibers were observed. In the electroacupuncture group, the density of fibers was intermediate compared with that in the sham-operated and SCI groups (**Figure 4**, **Table 3**).

Electroacupuncture improves nerve conduction in the injured spinal cord

Four weeks after SCI, SEPs and MEPs in the SCI group recovered slightly. SEP and MEP latencies were significantly shorter, and their amplitudes were significantly higher, in the electroacupuncture group compared with the SCI group ($P < 0.05$). There were significant differences in SEP and MEP latencies and amplitudes between the electroacupuncture and sham-operated groups ($P < 0.05$; **Table 4**).

Discussion

There is evidence that GFAP expression in the injured rat spinal cord is significantly decreased after electroacupuncture at the *Zusanli* (ST36) and *Huantiao* (GB30) acupoints on the hindlimbs in the rat, suggesting that electroacupuncture inhibits GFAP expression in astrocytes and promotes the recovery of axon function, thereby promoting spinal cord regeneration (Song et al., 2011). The possible mechanisms of action of electroacupuncture include: (1) inhibition of oxygen free radical formation and lipid peroxidation; (2) inhibition of apoptotic gene expression in neurons; and (3) increasing neurotrophic factor synthesis and receptor expression (Li et al., 2009). Winbeck et al. (2002) reported that electroacupuncture strengthens the recovery of Nissl body staining after SCI and promotes regeneration and repair.

Nogo protein activates Rho kinase and promotes C-reactive protein synthesis and secretion, resulting in neuronal cell loss. This persistent neuronal loss can lead to long-term, even permanent, neurological deficits (Lassmann et al., 2007). In this study, we assessed RhoA and Nogo-A mRNA and protein expression levels in injured spinal cord tissue and peripheral tissue using RT-PCR and western blot analysis. We found that (1) RhoA and Nogo-A mRNA and protein expression in the electroacupuncture group was significantly decreased 7 days after SCI, indicating that electroacupuncture alleviates SCI by downregulating RhoA and Nogo-A mRNA and protein expression; (2) the apoptotic index was decreased 4 weeks after SCI in the electroacupuncture group, demonstrating that electroacupuncture inhibits apoptosis; and (3) GFAP and NF-200 expression in the spinal cord in the electroacupuncture group was significantly increased, suggesting that electroacupuncture promotes neurophysiological recovery. Together, these results indicate that early electroacupuncture reduces neuronal cell death and decreases RhoA and Nogo-A mRNA and protein expression, and that delayed electroacupuncture increases GFAP and NF-200 expression in the injured spinal cord, thereby promoting regeneration and locomotor functional recovery following SCI.

In summary, electroacupuncture remarkably improves

the microenvironment in the injured spinal cord and plays an important role in alleviating secondary injury. Therefore, electroacupuncture may have substantial clinical potential for the treatment of SCI. Future studies are required to clarify the molecular and cell physiological mechanisms underlying the neurotherapeutic effects of electroacupuncture.

Author contributions: *MFW collected and integrated the data, wrote the paper, and authorized the study. RG conceived and designed the study, and was responsible for funding. SQZ analyzed the data. JBL performed statistical analysis. YL and QSZ provided technical assistance and guided the study. All authors approved the final version of this paper.*
Conflicts of interest: *None declared.*

References

Allen AR (1911) Surgery of experimental lesion of spinal cord equivalent to crush injury of fracture dislocation of spinal column. JAMA 57:878-880.

Davies SJ, Shih CH, Noble M, Mayer-Proschel M, Davies JE, Proschel C (2011) Transplantation of specific human astrocytes promotes functional recovery after spinal cord injury. PLoS One 6:e17328.

Ding Y, Yan Q, Ruan JW, Zhang YQ, Li WJ, Zeng X, Huang SF, Zhang YJ, Wang S, Dong H, Zeng YS (2011) Bone marrow mesenchymal stem cells and electroacupuncture downregulate the inhibitor molecules and promote the axonal regeneration in the transected spinal cord of rats. Cell Transplant 20:475-491.

Huang SF, Ding Y, Ruan JW, Zhang W, Wu JL, He B, Zhang YJ, Li Y, Zeng YS (2011) An experimental electro-acupuncture study in treatment of the rat demyelinated spinal cord injury induced by ethidium bromide. Neurosci Res 70:294-304.

Jiang W, Xia F, Han J, Wang J (2009) Patterns of Nogo-A, NgR, and RhoA expression in the brain tissues of rats with focal cerebral infarction. Transl Res 154:40-48.

Lassmann S, Schuster I, Walch A, Göbel H, Jütting U, Makowiec F, Hopt U, Werner M (2007) STAT3 mRNA and protein expression in colorectal cancer: effects on STAT3-inducible targets linked to cell survival and proliferation. J Clin Pathol 60:173-179.

Li HF, Jiang XH, Zou DQ, Cao QL, Lü J, Li Y, Zhang HF, Wang YP (2011) Expression of bone morphogenetic protein receptor IA in rats after contusive spinal cord injury. Nan Fang Yi Ke Da Xue Xue Bao 31:1124-1130.

Li K, Javed E, Scura D, Hala TJ, Seetharam S, Falnikar A, Richard J-P, Chorath A, Maragakis NJ, Wright MC, Lepore AC (2015) Human iPS cell-derived astrocyte transplants preserve respiratory function after spinal cord injury. Exp Neurol 271:479-492.

Li XN, Tian XS, Liu F (2009) Research on electric acupuncture on apoptosis related gene caspase-9 of rats spinal cord damaged. Zhongyiyao Xinxi 26:61-63.

Oyinbo CA (2011) Secondary injury mechanisms in traumatic spinal cord injury: a nugget of this multiply cascade. Acta Neurobiol Exp (Wars) 71:281-299.

Parikh P, Hao Y, Hosseinkhani M, Patil SB, Huntley GW, Tessier-Lavigne M, Zou H (2011) Regeneration of axons in injured spinal cord by activation of bone morphogenetic protein/Smad1 signaling pathway in adult neurons. Proc Natl Acad Sci U S A 108:E99-107.

Qiao HF, Lan BS, Liu YH (2008) Effects of electroacupuncture on the expressions of NF200 and GFAP in adult rats with spinal cord injuries. Zhongguo Kangfu Yixue Zazhi 23:635-637.

Song L, Li XN, Wang N, Wang WJ, Wang FY, Wang YW, Piao ZY (2011) Effects of electroacupuncture on expression of PARP-1 cleavage fragment after spinal cord injury of rats. Zhongyiyao Xuebao 39:86-88.

Wang D, Zhang JJ (2012) Electrophysiological functional recovery in a rat model of spinal cord hemisection injury following bone marrow-derived mesenchymal stem cell transplantation under hypothermia. Neural Regen Res 7:749-755.

Wang D, Zhang J (2015) Effects of hypothermia combined with neural stem cell transplantation on recovery of neurological function in rats with spinal cord injury. Mol Med Report 11:1759-1767.

Wang D, Fan YH, Zhang JJ (2013) Transplantation of Nogo-66 receptor gene-silenced cells in a poly(D,L-lactic-co-glycolic acid) scaffold for the treatment of spinal cord injury. Neural Regen Res 8:677-685.

Winbeck K, Poppert H, Etgen T, Conrad B, Sander D (2002) Prognostic relevance of early serial C-reactive protein measurements after first ischemic stroke. Stroke 33:2459-2464.

Xie J, Cheng YH, Zhu XH, Wan C, Yu XH (2013) Influence of electroacupuncture combined with magnetic stimulation therapy on AQP-4 and MCP-1 in model rat of spinal cord injury. Xiandai Zhongxiyi Jiehe Zazhi 22:2978-2979,3037.

Yang C, Ji L, Yue W, Wang RY, Li YH, Xi JF, Xie XY, He LJ, Nan X, Pei XT (2010) Erythropoietin gene-modified conditioned medium of human mesenchymal cells promotes hematopoietic development from human embryonic stem cells. Zhongguo Shi Yan Xue Ye Xue Za Zhi 18:976-980.

Copyedited by Patel B, Raye W, Yu J, Li CH, Song LP, Zhao M